coatings

MDPI

Article

Testing the Feasibility of Titanium Dioxide Sol-Gel Coatings on Portuguese Glazed Tiles to Prevent Biological Colonization

Mathilda L. Coutinho [1,2,*], João Pedro Veiga [3,4], Maria Filomena Macedo [1,4] and Ana Zélia Miller [2,*]

1 VICARTE, Research Unit Vidro e Cerâmica para as Artes, Faculdade de Ciências e Tecnologia, Universidade NOVA de Lisboa, 2829-516 Caparica, Portugal; mfmd@fct.unl.pt
2 HERCULES Laboratory and IIFA, University of Évora, 7000-809 Évora, Portugal
3 Centro de Investigação de Materiais, CENIMAT/I3N, Departamento de Ciência dos Materiais, Faculdade de Ciências e Tecnologia, Universidade NOVA de Lisboa, 2829-516 Caparica, Portugal; jpv@fct.unl.pt
4 Departamento de Conservação e Restauro, Faculdade de Ciências e Tecnologia, Universidade NOVA de Lisboa, 2829-516 Caparica, Portugal
* Correspondence: mathildal@gmail.com or magldc@uevora.pt (M.L.C.); anamiller@uevora.pt (A.Z.M.)

Received: 5 October 2020; Accepted: 26 November 2020; Published: 29 November 2020

Abstract: Historical glazed wall tiles are a unique vehicle of artistic expression that can be found outdoors, integrating the buildings of many countries, therefore they are often subjected to biodeterioration. In this work, the applicability of protective coatings on glazed tiles to prevent biological colonization was evaluated. Thin films of titanium dioxide (TiO_2) obtained by sol-gel were applied on glazed tiles to appraise its anti-biofouling properties and to evaluate their suitability for cultural heritage application. The TiO_2 coating was tested on four different Portuguese glazed tiles and a modern tile. The chemical and mineralogical characterization of the glaze and ceramic body of the tiles was examined by wavelength dispersive X-ray fluorescence spectroscopy (WDXRF) and X-ray diffraction (XRD). The produced TiO_2 coating was chemically and morphologically characterized by micro Raman spectroscopy (μ-Raman) and field emission scanning electron microscopy (FESEM). The anti-biofouling properties of the TiO_2 treatment were evaluated by inoculating the fungus *Cladosporium* sp. on the glazed tiles. Potential chromatic and mineralogical alterations induced by the treatment were assessed by color measurements and XRD. The TiO_2 coating did not prevent fungal growth and caused aesthetical alterations on the glazed tiles. A critical analysis evidenced that the tested coating was not suitable for cultural heritage application and highlighted the challenges of developing protective coatings for glazed tiles.

Keywords: cultural heritage; biodeterioration; biocides; ceramic glazed tiles

1. Introduction

Glazed wall tiles are ceramic plates covered with a vitreous glaze applied as revetment on buildings. As an integrated heritage, their uniqueness and artistic value result from the communion with the architectural structure for where they were originally designed [1]. Therefore, the displacement from their original location will influence their artistic and cultural value. When exposed outdoors, they are often susceptible to weathering [2–4] and biological colonization [3,5–10]. Complex microbial communities composed of bacteria, fungi, algae and cyanobacteria, have been identified on glazed tiles [3,5,7,8,10,11]. Aesthetical disfiguration is a conspicuous consequence of microbial growth [5,9,10,12]. Researchers have also reported other injurious effects, such as physical decay caused by the penetration of microorganisms

into fissures or underneath the glaze [5–7] and chemical decay associated with corrosion by metabolic substances [3,8], which could lead to irreversible losses.

Biodeterioration of outdoor built heritage assets is still an unsolved issue since environmental conditions and microorganisms cannot be controlled. Routine procedures for treating glazed tiles with biological colonization include mechanical cleaning (with brushes and scalpels) and biocides application to remove biofilms and inactivate microorganisms [13,14]. Several mechanical, physical and chemical methods have been tested for handling microbial growth on built heritage made of stone [15–19], but specific treatments for glazed tiles are scarce. Sparse studies tested thermal treatment, gamma radiation, commercial biocides and TiO_2 nanoparticles on tiles to inactivate and mitigate microorganisms [5,9,20]. Often, no long-term actions are foreseen, leading to recolonization after the treatment [5,21–23]. The need for recurrent interventions, besides costly, may have adverse side effects on the substrate. So, protective coatings could be a promising solution for glazed tile preservation. Coatings are currently applied on outdoor glazed tile interventions mainly to improve water repellence and delay deterioration processes. Different materials are thus selected for these purposes, such as organic resins (acrylic, epoxydic, polyester, vinylic, polyurethane), microcrystalline waxes, siloxanes and other hybrid polymers [24–29]. Many of these materials have a low resistance towards outdoor conditions [29] and can even encourage colonization by microorganisms (increasing bioreceptivity [30]) [10]. An experimental study tested applying TiO_2 and SiO_2 thin films by ion plating plasma on historical tiles, but their efficacy or harmfulness was not evaluated [31]. Protective coatings have been widely researched for their application on glass cultural heritage due to its propensity to corrosion. Studies included SiO_2 sol-gel and nanocomposite coatings, showing good properties for preventing the glass corrosion on stained glass, glass mosaic tesserae and glass models with chemical compositions based on historical glasses [32–35]. However, some of these studies reported that the coatings were visible at naked eye [34,36]. Neither the coatings tested on glass nor glazes were evaluated regarding anti-biofouling properties.

TiO_2 nanoparticles are the most studied photocatalytic materials for preventing biological colonization of cultural heritage [37,38]. The TiO_2 anti-biofouling properties result from the photocatalytic effect, which generates free radicals and hydrogen peroxide when irradiated with UV-light (bandgap energy of 3.2 eV, circa λ = 388 nm) [39]. On the one hand, these free radicals attack cell walls and cell structures, resulting in microbial growth inactivation [40]. On the other hand, TiO_2 creates a self-cleaning surface due to its photoinduced superhydrophilicity (water contact angle close to 0°). A thin water film is formed on the surface, avoiding dirt and microorganisms accumulation [41]. Different methods have been attempted to impart anti-biofouling properties to built heritage structures with TiO_2 nanoparticles [42–44]. The simplest method has been tested on several substrates, including on historical glazed wall tiles. It consists of applying nanoparticles in solvent suspension directly on the surface [5,42,45–48]. Several TiO_2 coatings of diverse nature (organic, inorganic and hybrid) have also been described in literature reviews on TiO_2 materials for cultural heritage applications [37,43]. Sol-gel is probably the most straightforward method for producing these coatings in terms of required equipment, low-temperature processing, and good results regarding film properties (homogeneity and purity) [35,43]. The method involves a two-step reaction: hydrolysis and condensation. First, the metal alkoxides (Ti-OR in the case of TiO_2 or Si-O in the case of SiO_2) react with water through a hydrolysis reaction resulting in the replacement of the alkyl group. Then, condensation occurs, forming amorphous hydroxides (M-O-M bonds). Thermal treatment of the film might be necessary for densification, obtain the desired crystalline phase, and increase adhesion with the substrate. Diverse formulations have been evaluated for cultural heritage application: TiO_2, doped TiO_2, nanocomposite coatings with SiO_2 and TiO_2 and hybrid coatings. Doping TiO_2 with other ions, such as Fe, Cu, Ag, S, N and C, is a common solution to overcome the need for UV-light and extend the photocatalytic activity into the visible spectral range [43]. However, the absorption in the visible region causes coloration [47,49]. A review on TiO_2 nanocoatings for cultural heritage applications concluded that doped coatings usually induced higher chromatic variations [43]. Recent studies have

emphasized that the substrate properties, particularly high roughness and porosity, also influence the treatment's efficacy [50,51]. One of the advantages of the TiO_2 applied as coatings is the immobilization of the nanoparticles on the surface, avoiding their penetration and reducing leaching. The impact of nanoparticles on the environment following leaching from treated surfaces is an actual concern due to the lack of ecotoxicity data [12]. The aging of coatings and consequent loss of their properties are also a major concern that has been described in several works [52,53]. In addition, some of these novel coatings are still not adapted for in-situ application due to the complexity of the depositional procedures required for the application of TiO_2 coatings [31]. However, many tile interventions, such as desalinization treatments, replacement of mortars, and stabilization of the building structures, involve the removal of tiles, which would allow an appropriate application of these coatings before the remounting of the tiles onto the original location. Yet, it is important to emphasize that the efficacy of any treatment on cultural heritage assets must comply with several requirements, specifically: (i) harmless and compatibility with the substrate; (ii) long-term stability; (iii) reversibility (or at least retractability); (iv) environmental sustainability, and (v) aesthetical compatibility [37,54].

The functionalization of glazed surfaces for several purposes (self-cleaning, anti-fouling or antimicrobial) is well-established in the field of building materials, but not on historical glazed tiles [55]. In Europe, lead glazes (such as tin-opacified, lead-alkali or high lead silicate glazes) were mainly applied to produce historical tiles [56–58], which are very different from the lead-less chemical compositions of modern glazes. Lead glazes tend to be susceptible to acidic corrosion, causing lixiviation of lead and other ions [32,59]. Thus, the reproduction of historical materials might not mimic the complexity of aged surfaces. The applicability of these coatings on historical tiles must be evaluated to understand if these promising treatments can be a solution to protect them against biodeterioration.

In this work, the feasibility of applying photocatalytic TiO_2 coatings on historical glazed tiles to prevent biodeterioration was evaluated. The deposited sol-gel thin-films were characterized by μ-Raman for mineralogical analysis and field emission scanning electron microscopy (FESEM) for morphological characterization. The efficacy of the TiO_2 coatings on glazed tiles for preventing microbial growth was evaluated through bioreceptivity tests by inoculating the fungus *Cladosporium* sp. and further evaluating fungal growth. The harmfulness of the treatment on historical tiles was appraised regarding its aesthetical alteration visually and by measuring chromatic variation. Additionally, the mineralogical composition of the tile's ceramic body was investigated after the treatment. The results were then critically assessed, considering the specific requirements for cultural heritage application.

2. Materials and Methods

2.1. Tile Samples

Four types of tile substrates were selected for sol-gel thin coatings deposition (samples 1BW, 2W, 3TS and 4MW). The set of tiles was selected to represent different production techniques: a hand-painted blue and white earthenware tile (1BW), a semi-industrial stencil decorated tile (2W), a white industrial earthenware tile (3TS) and a modern tile (4MW). The details of the tile samples used in this work are summarized in Table 1. The tiles comprised damaged fragments without known provenance and did not evidence any previous degradation, such as biological colonization, salt damage, or corrosion. Samples 1BW, 2W and 3TS were obtained from a deposit of construction materials from demolished buildings and 4MW is an industrial modern white tile. The tiles were cut into pieces with circa 1.5×3 cm^2. Before the coating application, glaze surfaces were cleaned with ethanol and rinsed with distilled water. Small samples of the ceramic body were cut into smaller pieces (10 mm × 10 mm) for compositional analysis and harmfulness testing.

Table 1. Description of the tile samples selected for the experiment.

Ref.	Tile Description
1BW	Blue and white majolica tile. Possibly dating from the 18th or 19th century.
2W	Green and white tile decorated with stencil. Possibly dating from the late 19th or early 20th century. Solely white areas of the tile were selected for analysis.
3TS	Transparent glazed tile. Early 20th century tiles from the Sacavém Ceramic Factory (Portugal).
4MW	Modern industrial white tile.

2.2. Tile Characterization

Elemental analysis of the tiles' ceramic body and glaze was conducted by wavelength dispersive X-ray fluorescence spectrometry (WDXRF). The analyses were performed with a PANalytical XRF-WDS 4 kW AXIOS (PANalytical B.V., Almelo, The Netherlands) sequential spectrometer using a Rh X-ray tube and an He flow. Spectra deconvolution by the iterative least-squares method and standardless semi-quantitative analysis based on the fundamental parameter approach were carried out with the SuperQ IQ+ software package (PANalytical B.V., Almelo, The Netherlands). The glaze was analyzed directly over the tile samples and the ceramic body was separated from the glaze and ground into a fine powder. For accuracy purposes, the lead-silicate reference glass Corning Museum of Glass C (CMOG C) was also analyzed.

2.3. Synthesis and Application of TiO_2 Coatings

Sol-gel was prepared according to a previously described procedure [60] using the following reagents without further purification: Titanium (IV) isopropoxide (Sigma-Aldrich, St. Louis, MO, USA, 99.9%) as the precursor, ethanol (CH_3OH) (Sigma-Aldrich, Puriss p.a) and acidic water (HNO_3). Sol was refluxed for 48 h at 85 °C. The superficial liquid phase was collected and separated from the white deposit formed after the refluxing process was obtained. The sol (pH 1.25) was deposited on the tile samples through the Spincoat G3P–8 (Special Coating Systems, SCS) device at a speed of 2500 rpm/s to ensure reproducibility. Samples were air-dried for 24 h prior to thermal treatment. Tiles with air-dried coatings were annealed on the furnace at 350 °C for 4 h. The thermal treatment was necessary to crystallize the amorphous TiO_2 thin-film into the anatase phase.

2.4. Characterization of TiO_2 Thin Film

μ-Raman was performed to analyze the crystallinity of the TiO_2 thin film with a Labram 300 Jobin Yvon spectrometer, equipped with a He-Ne laser of 17 mW power operating at 632.8 nm and also a solid-state external laser of 50 mW power operating at 514.5 nm. Spectra were recorded as an extended scan and the laser beam was focused with 100× Olympus objective lens. The laser power at the surface of the samples varied with the aid of a set of neutral density filters of 0.6.

Surface morphology, thickness and the interface between the glaze and the deposited thin films were observed by field emission scanning electron microscopy (FESEM). The analysis was carried out with a Jeol JSM-7001F microscope equipped with an Oxford EDS light elements detector for chemical analysis using secondary X-rays and standard ZAF corrections that allow semi-quantitative microanalysis. Tile samples were previously sputter-coated with a thin gold/palladium film.

2.5. Tertiary Bioreceptivity Experiment

A set of non-treated tile samples (n = 3) and a set of TiO_2-treated samples (n = 3) were selected for a tertiary bioreceptivity experiment (Figure 1). The selected fast-growing fungus *Cladosporium* sp. was previously isolated from a biological patina growing over the majolica glazed tiles from Pena National Palace, Portugal [61]. The fungus was grown in potato dextrose agar (PDA) plates at room temperature. For the inoculum, the fungal strain was scraped from 1 cm^2 of the PDA plates with a sterile scalpel and suspended in dilute PDA liquid medium (10 g/L) (Scharlau, Barcelona, Spain).

On the inoculation day, each set of tiles were placed inside a glass Petri dish suspended over a net with distilled water at the bottom. Non-treated and TiO_2-treated samples of each tile were placed in the same Petri dish. Before the inoculation, Petri dishes containing the tile samples on the top of a net and water at the bottom were sterilized (autoclaved at 120 °C at 100 kPa above atmospheric pressure for 20 min). After slow cooling at room temperature, 150 µL of fungal suspension was inoculated on the center of each tile sample. All tile samples were kept outdoors on the terrace of a building situated in Almada (Portugal) exposed to direct sunlight for 40 days (March to April). The climatic conditions were characterized by mild temperatures with an average day temperature of circa 14–16 °C. The water at the bottom of the Petri dishes was periodically re-filled. Fungal growth was studied through photographic documentation at four different incubation times: 0 (t = 0), 10 (t = 10), 20 (t = 20) and 40 days (t = 40). The recorded images were then treated by digital image analysis using Photoshop CS6 and MATLAB software to determine the percentage of the colonized area (Equation (1)):

$$\%\text{colonized area} = (\text{nr. of colonized pixels} \times 100)/\text{nr. pixels tile area} \quad (1)$$

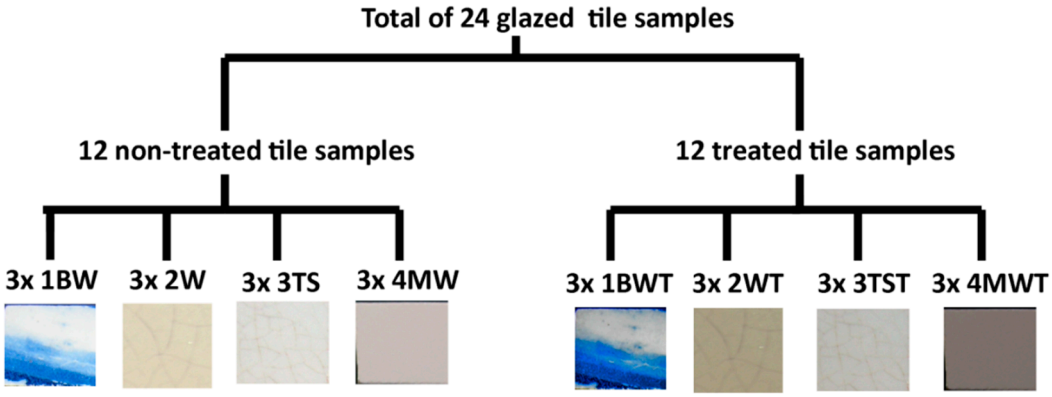

Figure 1. Scheme with experimental design with the number of replicates of non-treated (1BW, 2W, 3TS and 4MW) and TiO_2-treated (1BWT, 2WT, 3TST and 4MWT) samples.

2.6. Characterization of Tiles before and after Treatment

Macroscopic observations were performed by visual inspection and photographic documentation before and after the coating application with an Olympus C-5060 digital camera (Olympus Europa SE & Co. KG, Hamburg, Germany). A Kodak Color scale was included in each record for light and color adjustment of the images.

The aesthetic effect of the TiO_2 coating on tile samples was also evaluated by UV–Visible diffuse reflectance. The spectra were collected with a Shimadzu UV-2501PC spectrometer directly on the surface of the tiles using an integrating sphere and $BaSO_4$ as a reference. Spectra were then converted into chromaticity values defined by CIELAB coordinates UV-2501 PC Colour Analysis software. The color was defined through three different parameters, L^*(brightness), a^*(red/green) and b^*(yellow/blue). To assess the chromatic alteration caused by TiO_2 coatings, the tile surfaces were analyzed before and after coating deposition. The variation between the treated and original were calculated for each parameter (ΔL^*, Δa^* and Δb^*), and total color difference (ΔE^*) with the following equation (Equation (2)):

$$\Delta E^* = \sqrt{\left[\left(\Delta L^*\right)^2 + \left(\Delta a^*\right)^2 + \left(\Delta b^*\right)^2\right]} \quad (2)$$

X-ray diffraction (XRD) analysis of the powdered ceramic body was performed for mineralogical characterization. After treatment (coating deposition and thermal treatment), XRD was performed to detect possible induced alterations on the mineralogical composition of the ceramic body due to the TiO_2 treatment. The XRD patterns were recorded on a Rigaku Dmax III-C 3 kW diffractometer (Rigaku Corporation, Tokyo, Japan), using the following operating conditions: Cu Kα radiation at 40 kV

and 30 mA in the 2θ ranging from 20° to 80°, and an acquisition time of 1 s and 2θ increment of 0.08°. The EVA software (Bruker AXS GmbH, Karlsruhe, Germany) was used for spectral deconvolution and mineral phase identification compared with standard files (ICDD, Newtown Square, PA, USA).

Considering that the 1BW tile samples showed dark stains on the surface after TiO_2 coating application and thermal treatment, further analyses were performed to investigate this alteration. Small fragments of these tiles were exposed to HNO_3 solution, with pH = 1.25 (equal to the prepared sol-gel) for 2 h by placing a soaked cotton swab over the glazed surface. Scanning electron microscopy with energy-dispersive X-ray spectroscopy (SEM-EDS) examinations were conducted for investigating the morphological alteration of the surface after exposure. These tile samples were directly mounted on sample stubs, sputter-coated with gold and examined on a Hitachi 3700 N SEM (Hitachi, Tokyo, Japan) interfaced with a Quantax EDS microanalysis system (Bruker AXS GmbH, Karlsruhe, Germany). The Quantax system was equipped with a Bruker AXS XFlash Silicon Drift Detector (129 eV spectral resolution at full width at half maximum—Mn Kα). The operating conditions were backscattered electron mode, 20 kV accelerating voltage, 10 mm working distance and 120 mA emission current.

3. Results

3.1. Chemical Composition of Tile Glaze and Ceramic Body

The chemical composition of the glaze and ceramic body of the tile samples obtained by WDXRF are shown in Table 2. The main components of the glaze tile samples 1BW, 2W and 3TS were SiO_2 and PbO, with values ranging between 60–70 and 14–17 wt.%, respectively. The content of alkalis (Na_2O and K_2O) was higher for sample 1BW, followed by sample 2W and 3TS. Glaze 1BW depicted the lowest content of Al_2O_3 of the three historical glazes and 3TS the highest content with 10 wt.%. On samples 1BW and 2W, the calcium content was lower than the glaze of the 3TS sample (Table 2). SnO_2 (5 wt.%) was detected on the glaze of 1BW and 2W samples; both are opaque white glazes opacified with SnO_2. On sample 1BW, taken from a blue and white tile, cobalt was also detected (Table 2). The major components of the tile glaze 4MW were SiO_2, Al_2O_3 and CaO. This glaze belongs to a modern industrial tile, which differed significantly from the historical glazed tiles (1BW, 2W and 3TS), particularly by the absence of lead and tin. A high percentage of ZrO (3 wt.%) was detected on the 4MW glaze since this was probably used as an opacifier.

Table 2. Major and minor oxide components of the glaze and ceramic body of the tile samples in wt.(%).

Sample	1BW		2W		3TS		4MW		CMOG C	
Area	**G**	**CB**	**G**	**CB**	**G**	**CB**	**G**	**CB**	**Meas**	**Ref**
Na_2O	4	<1	1	<1	<1	<1	1	1	1	1.07
Al_2O_3	3	8	4	11	10	21	14	22	0.9	3
SiO_2	60	39	71	57	66	73	67	62	45	34.8
K_2O	5	1	3	2	4	2	3	3	3	2.84
CaO	1	45	1	22	5	<1	9	9	6	5.07
TiO_2	<1	1	<1	1	<1	<1	<1	<1	0.9	0.79
Fe_2O_3	1	5	1	5	1	1	1	1	0.6	0.34
CoO	2	–	–	–	–	<1	–	–	0.2	0.18
ZrO	–	–	–	–	–	–	3	<1	–	–
SnO_2	5	–	5	–	–	–	–	–	0.4	0.19
PbO	17	<1	14	<1	15	<1	<1	<1	27	36.7

G—Glaze; CB—Ceramic body; Meas—Measured; Ref—Reference composition; <1—<1 wt.%.

The ceramic body of the tile samples 1BW and 2W were rich in SiO_2 (39 and 57 wt.%, respectively) and CaO (45 and 22 wt.%) (Table 2), with similar contents of Al_2O_3 (8 and 11 wt.%) and Fe_2O_3 (5 wt.%). The ceramic body of samples 3TS and 4MW showed lower contents of CaO (bellow 1 and 9 wt.%) and Fe_2O_3 (1 wt.%) and were richer in Al_2O_3 (21 and 22 wt.%) (Table 2).

3.2. Characterization of TiO_2 Thin-film

3.2.1. μ-Raman Analysis

Raman spectra obtained directly on the coated tile surfaces revealed spectral features corresponding to the anatase polymorphic phase of TiO_2. Figure 2 displays a spectrum obtained on sample 3TS, showing the banding pattern of anatase with a slight shift from assignments made in the literature [62]: 146 cm^{-1} (B1g mode, very intense), 198 cm^{-1} (Eg mode, very weak), 400 cm^{-1} (B1g mode, intense), 516 cm^{-1} (A1g, B1g modes, less intense) and 634 cm^{-1} (Eg mode, less intense).

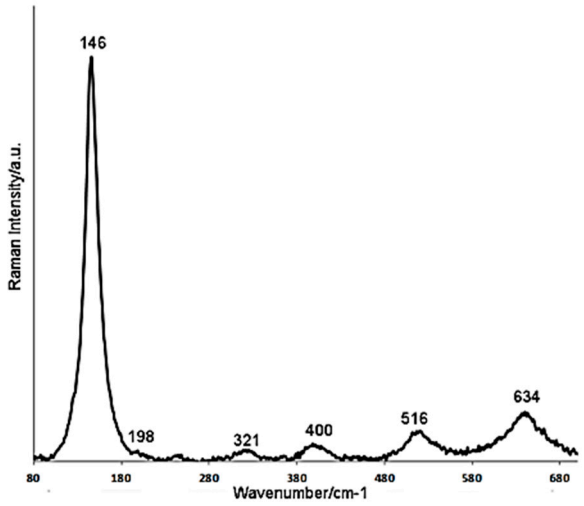

Figure 2. Representative Raman spectrum of TiO_2-coatings. Example of anatase Raman spectrum collected from the thin film deposited on a 3TS sample.

3.2.2. Morphology of the TiO_2 Coating

SEM images revealed that the TiO_2 film completely coated the surface of the glazed tiles (Supplementary Materials Figure S1). Nevertheless, existing fissures on the glaze could still be observed on the coated tile samples 1BWT and 3TST (Figure S1). The surface morphology of the applied TiO_2 coating was also investigated by FESEM (Figure 3). The TiO_2 coating formed a crack-free thin film over the glazed surface. At lower magnification, a homogeneous thin-film with larger particles dispersed on the surfaces were observed on all types of tile (Figure 3a–d). The TiO_2-coated 1BWT sample showed a few dispersed pores (Figure 3a), but less surface particles in comparison with other samples (Figure 3b–d). At higher magnification, the nanostructure of the thin film was similar for all tile samples, with small agglomerates of cauliflower-like structures distributed over the surface (Figure 3e–h). The grain size of the TiO_2 coating was not measured, but at higher magnifications, it is possible to infer that it is in the nanometric scale (Figure 3e–h). Additionally, details of the microstructure of the glaze were observed by SEM and FESEM examinations. Dark and light-colored areas were observed on the glazed surface of samples 2WT (Figure 3b,f) and 1BWT (Figure S1), which could be related to the presence of inclusions richer in elements with lower (dark areas) or higher atomic number (light areas).

FESEM investigations allowed observing the thin film section and measuring the thickness of the TiO_2 coating, which was 60–89 nm (Figure 4). FESEM images of the tile sections revealed good adherence of the TiO_2 coating to the glazed surface for all tile samples (Figure 4). A well-defined interface between the glaze and the TiO_2 coating could be observed, with no evident signs of a corrosion layer underneath the coating.

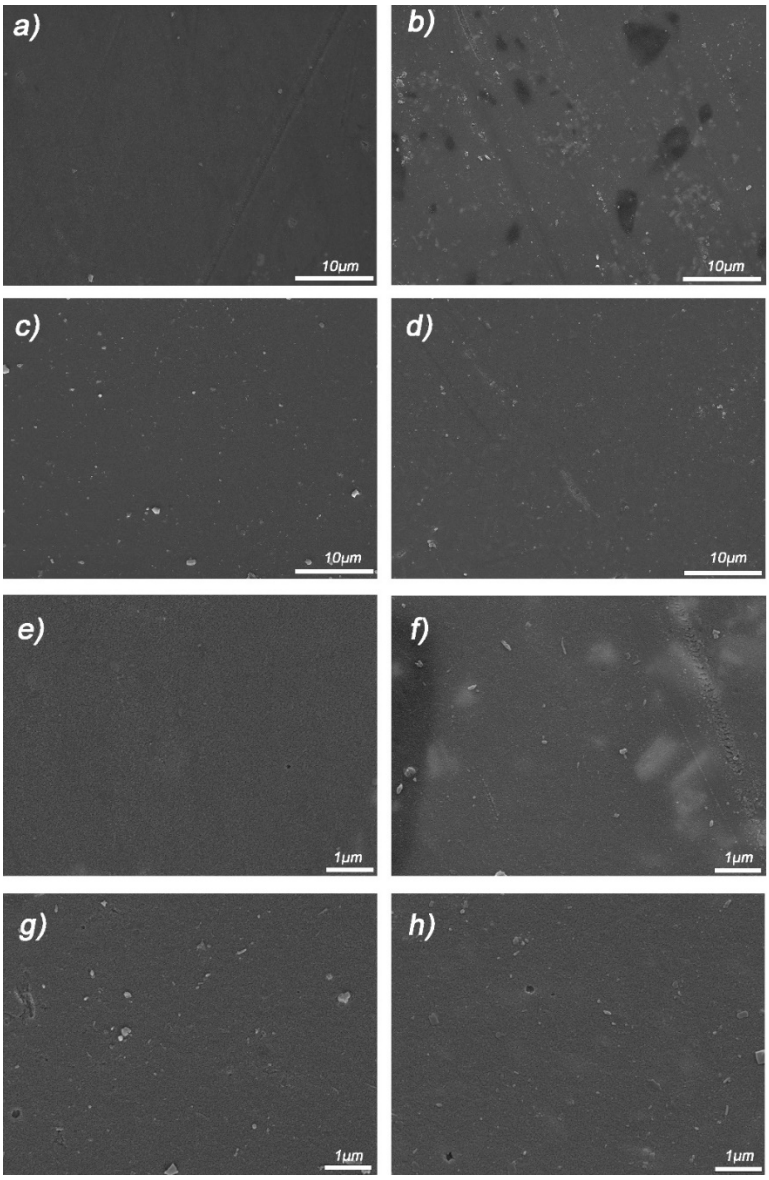

Figure 3. Field emission scanning electron microscopy (FESEM) images of the TiO_2-coated glazed surfaces. Surface of: (**a**) tile 1BWT, (**b**) tile 2WT, (**c**) tile 3TST and (**d**) tile 4MWT. Higher magnification images of TiO_2 coating on: (**e**) 1BWT, (**f**) 2WT, (**g**) 3TST, and (**h**) 4MWT.

3.3. Tertiary Bioreceptivity Experiment

Throughout 40 days of incubation, photographic documentation showed fungal growth on the non-treated and treated samples (Figure 5). The results showed that the fungal growth rate was faster for the first 10 days of incubation. There was no significant growth between the 10th and the 20th days of incubation or between the 20th and 40th days, confirming the stagnation of the fungal growth (Figure 5).

Digital image analysis was performed to quantify the percentage of the tile surface that was colonized by the fungus *Cladosporium* sp. (Figure 6). Fungal proliferation over the tile surfaces was more extensive on samples 4MW and less abundant on sample 3TS. In general, the comparison between the non-treated and TiO_2-treated tiles showed that fungal proliferation was higher on the non-treated samples (Figure 6). The only exception was observed on 4MW samples, where the treated tiles (4MWT) showed higher fungal proliferation, reaching values close to 40% (Figure 6).

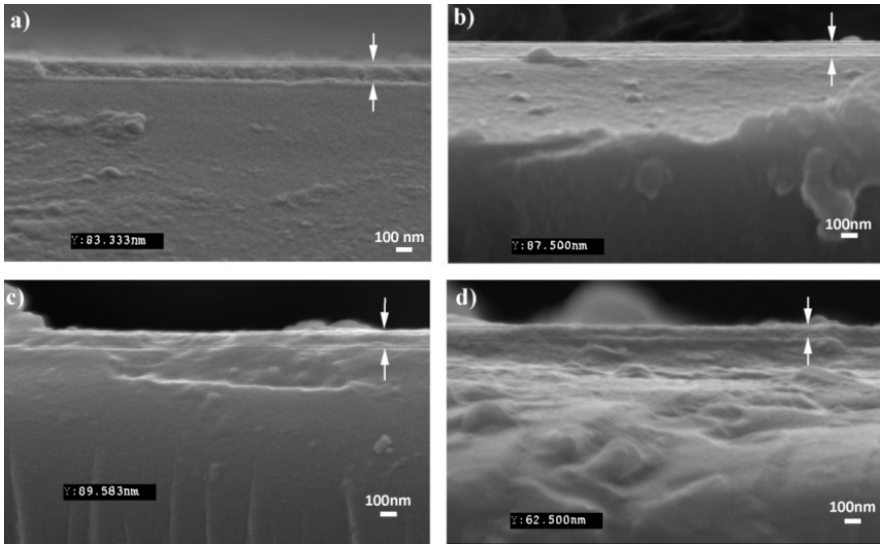

Figure 4. FESEM images of cross-sections of the coated tile surfaces with arrows indicating the TiO_2 coating and Y value showing the measurement of the thickness of the thin film. (**a**) Sample 1BWT with Y = 83.33 nm, (**b**) sample 2WT with Y = 87.500 nm, (**c**) sample 3TST with Y = 89.583 nm, and (**d**) sample 4MWT with Y = 62.500 nm.

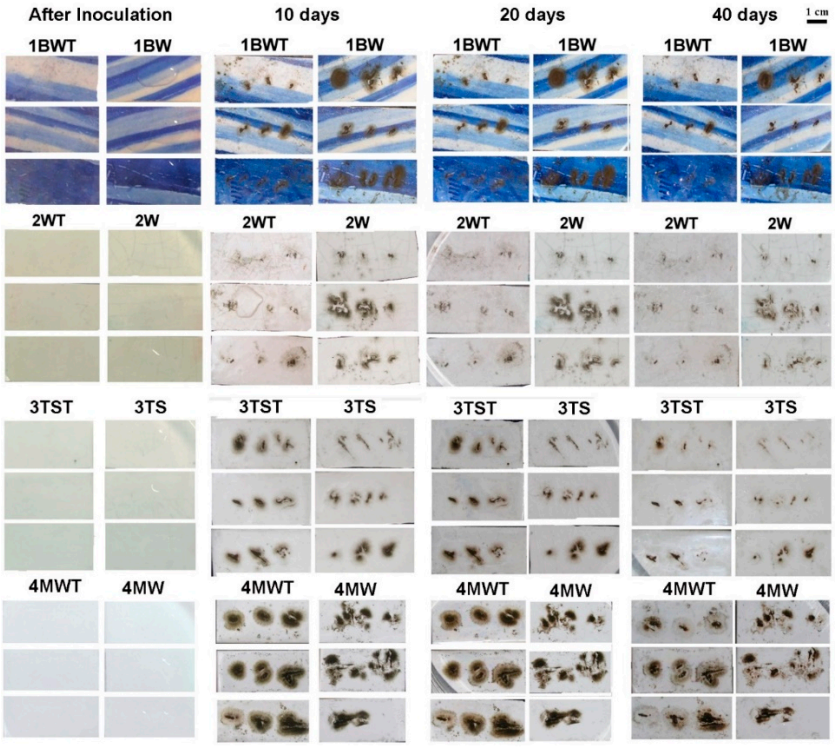

Figure 5. Photographic documentation made during the experiment of the fungal growth on glaze tile samples 1BW (non-treated); 1BWT (TiO_2-treated); 2W (non-treated); 2WT (TiO_2-treated); 3TS (non-treated); 3TST (TiO_2-treated); 4MW (non-treated) and 4MWT (TiO_2-treated) at four different stages: after inoculation, after 10 days incubation, after 20 days incubation and after 40 days incubation. Scale bar: 1 cm.

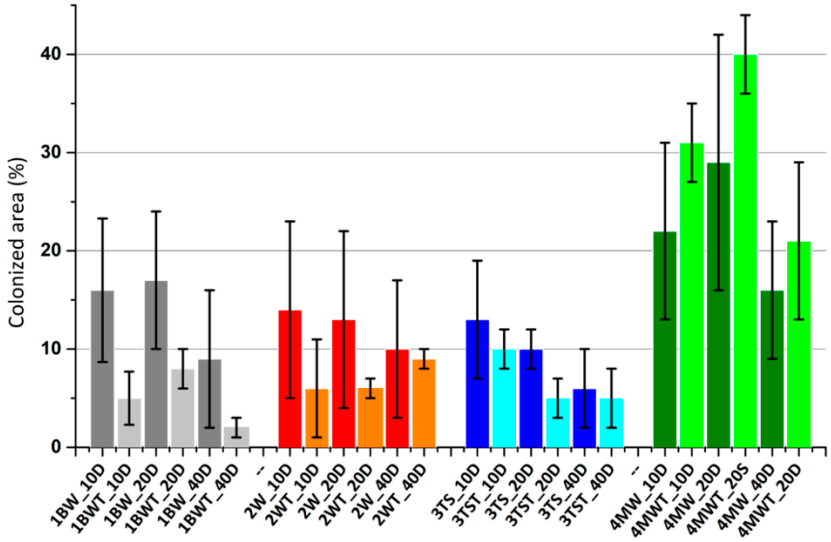

Figure 6. Average percentage and standard deviation of tile surface (%) colonized by the fungus *Cladosporium* sp. on non-treated (n = 3, darker color) and TiO_2-treated (n = 3, lighter color) tiles obtained by digital image analysis after 10-, 20- and 40-days incubation.

3.4. Evaluation of the Chromatic Alteration Caused by Thin-Film Deposition

Visual inspection and photographic recording were performed before and after the coating application to observe possible aesthetical alterations. The major change that occurred on all the samples due to the application of the TiO_2 coating was the iridescent effect of the surface, particularly conspicuous when observed under oblique angles (Figure 7a,b). Despite this effect being similar on all tile surfaces, it was difficult to document by photographic recording (Figure 7a,b).

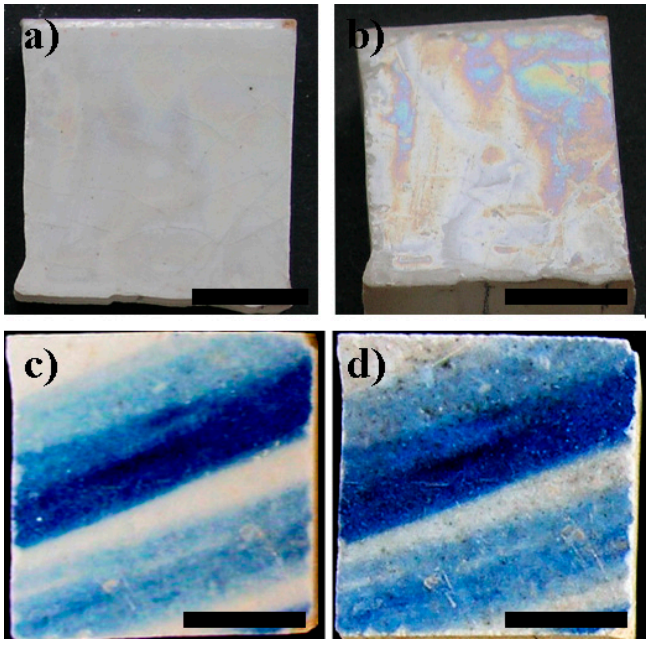

Figure 7. Aesthetical interference of the TiO_2 coating. (**a**) Sample 3TS photographed from a straight angle (90°); (**b**) Iridescent of the TiO_2 coating applied on tile sample 3TS observed from an oblique angle. Tile 1BW (**c**) before TiO_2 and (**d**) staining and darkening of the surface after the application of TiO_2 coating. Scale bars: 1 cm.

On tile sample 1BW, the iridescent effect was accompanied by the darkening of the surface and grey stains formed underneath the coating (Figure 7c,d). The stains were only visible on this tile type; none of the other samples showed this effect after the coating application. The dark stains could not be identified by μ-Raman. To understand if the blacking was caused by the acidic effect of the TiO_2 sol-gel, non-treated 1BW samples were exposed to HNO_3 solution with pH 1.25, which was the same pH as the applied sol-gel. At naked eye, the samples did not show any signs of corrosion or blackening. SEM observations of these tile surfaces revealed small deposits, probably of corrosion products. Neither pitting nor cracking was detected on the surface of the tested tiles (Figure S2).

Chromatic changes caused by the coating application and the thermal treatment were analyzed by color measurements using the CIELAB coordinates (Figure 8). The ΔE^* obtained before and after the application of the coating varied between 3.38 and 5.93. These values resulted from the variation of the luminosity parameter (ΔL^*), which was considerably higher than the variation of the chromaticity expressed in $\Delta a^*$and Δb^* (Figure 8). The b^* parameter of all tile samples decreased, which reflects a shift towards the blue color.

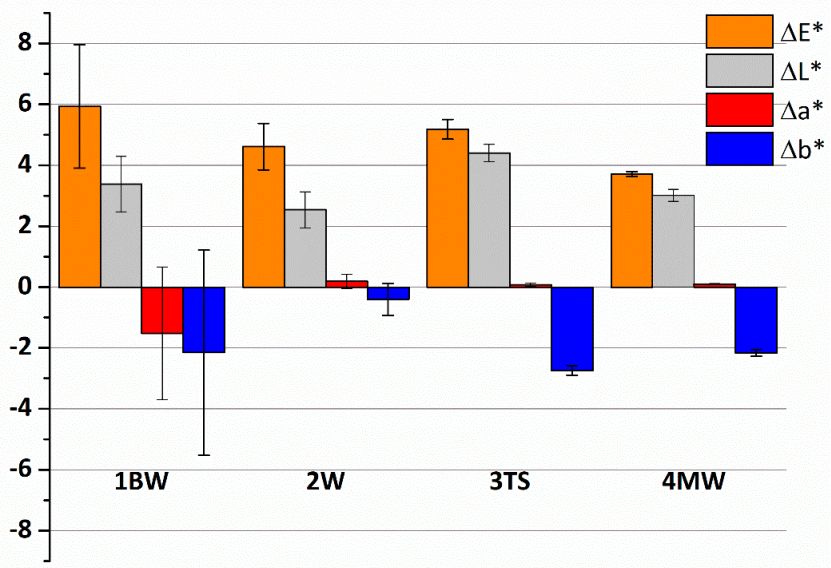

Figure 8. Colorimetric variation before and after the coating application expressed as ΔE^*, ΔL^*, Δa^* and Δb^*.

3.5. XRD Analysis

XRD results revealed that the ceramic body of sample 1BW contained quartz (SiO_2), calcite ($CaCO_3$), gehlenite ($Ca_2Al_2SiO_7$), äkermanite ($Ca_2Mg{\cdot}Si_2O_7$) and wollastonite ($CaSiO_3$) (Figure 9). The mineralogical composition of sample 2W was similar regarding the detected mineral phases, but the Ca-bearing phases presented less intense bands (Figure 9a). Quartz was the most prominent peak on sample 2W (Figure 9b), instead of calcite and gehlenite that were the main phases in sample 1BW (Figure 9a). Quartz (SiO_2) and mullite ($3Al_2O_3{\cdot}2SiO_2$) were the mineral phases detected in sample 3TS (Figure 9c). XRD revealed quartz (SiO_2) as the most prominent phase, as well as albite ($NaAlSi_3O_8$) in sample 4MW (Figure 9d). The analysis performed on the ceramic body after thermal treatment to evaluate the effect of the film application suggested that no significant changes occurred in the crystalline phases of the tiles.

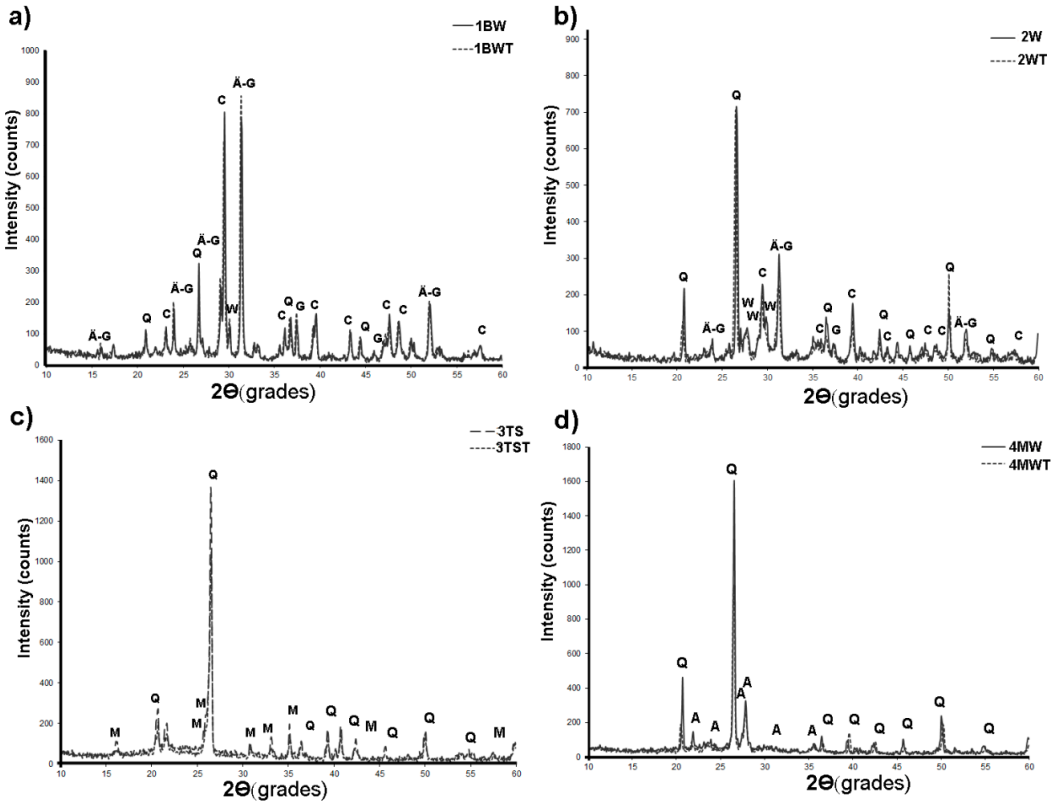

Figure 9. X-ray diffraction patterns of the ceramic body before and after the treatment: A—albite, C—calcite, G—gehlenite, Q—quartz, M—mullite, W—wollastonite and Ä—äkermanite. Diffractogram of ceramic body of the tile: (**a**) 1BW (before—1BW and after—1BWT); (**b**) 2W (before—2W and after—2WT); (**c**) 3TS (before—3TS and after—3TST); and (**d**) 4MW (before—4MW and after—4MWT).

4. Discussion

The reproduction of tiles can be difficult due to the innumerous variables involved in the ceramic production process, such as granulometry, nature of raw materials, and firing (cycle, temperature and atmosphere). However, TiO_2-coated tiles are already a market product with good results in modern tiles [55], which significantly differ from historical tiles. Therefore, real tile samples were selected to evaluate the application of the coatings on historical glazed tiles with diverse compositions and that were naturally weathered. The use of authentic materials for testing conservation treatments can be controversial, yet many studies have adopted this approach by employing test subjects (tiles without specific cultural value) due to the constraints mentioned above [63–66].

4.1. Tile Samples

The surface of tile 1BW showed a continuous glaze without a regular network of cracks (Figure 1). The glaze sample 1BW, taken from a blue and white majolica tile, was a lead-alkaline silicate glaze opacified with SnO_2 (Table 2). Pereira et al. [67] and Coutinho et al. [5] also characterized blue and white tiles with similar stylistic features [68] and obtained compositions similar to tile 1BW, with Si, Pb and Sn as main components. The ceramic body of sample 1BW showed a Ca-rich composition (Table 2), as well as mineral phases commonly found on ceramic bodies with high Ca content, such as gehlenite, wollastonite and anorthitic plagioclases (Figure 9). These minerals are formed when the firing temperature is above 950 °C during the ceramic production process [69]. After firing, the presence of calcite can be related either to low firing temperatures, high rates of Ca/Si ratio or degradation of calcium phases [70]. Regarding the glaze's morphology, some disperse micro-fissures were observed on the surface of the glaze (Figure S1). SEM analysis revealed some micro-fissures formed around

dark inclusions (Figure S1a), probably composed of quartz. Similar micro-fissures were previously observed on majolica glazed tiles from the Casa da Pesca Manor House [5]. These may be attributed to production flaws caused by the different behavior of glass and quartz inclusions during firing.

The glaze of sample 2W depicted cracks visible by the naked eye (Figure 1), which can occur due to production flaws and aging processes [71]. Sample 2W has a lead-alkaline silicate glaze opacified with SnO_2, typically employed on the majolica technique. The ceramic body had a lower content of CaO and a higher Al_2O_3 content than sample 1BW (Table 2). The numerous Ca-bearing phases detected by XRD, such as calcite, gehlenite, äkermanite and wollastonite (Figure 9), corroborate the relatively high Ca content. This mineralogy was similar to the ceramic body of the blue and white tile (1BW). In fact, both tiles showed a similar type of glaze and ceramic body. However, based on stylistic features [68] and particularly the stencil decoration of tile 2W, we can consider that 2W tiles correspond to a more recent production than 1BW. The 2W tiles are probably pre-industrial tiles, which were used for claddings produced during 1840–1920 [68]. The SEM analysis performed for characterizing the TiO_2 coating revealed dark and light-colored inclusions, which could be composed of quartz and tin-oxide, respectively (Figure 3b,f and Figure S1b).

The 3TS tile showed a glaze layer with a well-defined crack network visible by the naked eye (Figure 1). The regular crack network is typical of white fine earthenware ceramics due to the ceramic body's porosity and its tendency to expand due to hydration with the aging process. Sample 3TS was taken from a tile produced in the Sacavém's ceramic factory (Portugal) at the beginning of the 20th century. This showed a lead silicate glaze rich in CaO without any opacifying compound. The glaze was applied over a white industrial earthenware body rich in SiO_2 and Al_2O_3. The ceramic body was fired at high temperatures since quartz and mullite were the main mineral phases detected on the tile samples 3TS. Mullite is formed on ceramic bodies with low content in CaO [72]. The composition of the ceramic body is in fair agreement with the notes on ceramic paste recipes presented in the catalogue of the Museu da Cerâmica de Sacavém, which described the use of kaolin, ball clays, feldspars and small amounts of cobalt oxide [73]. In fact, cobalt was also detected as a minor element in tiles 3TS (Table 2).

The glaze of 4MW tile was smooth and no surface flaws were visually detected on the tile surface (Figure 1). This modern industrial tile (4MW) showed a ZrO opacified glaze which is today the most used opacifier. The ceramic body composition comprised a modern ceramic paste with low calcium oxide content and a high content of alumina and silica, commonly reported in modern tile compositions [74].

In conclusion, the four types of ceramic tiles studied showed different compositions and physical features. The three historical tiles had considerable amounts of lead in the glaze composition; only the modern tile did not present lead in its glaze. Nowadays, lead oxide can no longer be used in high amounts due to its toxicity [75]. Additionally, their physical features showed differences, particularly in the extents of micro-fissures or cracks: the modern tile showed a flawless surface (4MW), sample 1BW displayed dispersed micro-fissures and samples 2W and 3TS a regular network of cracks visible at naked eye. Therefore, an increasing permeability from 4MW < 1BW < 2W/3TS can be expected, as the higher the number of breakages (micro-fissures or cracks) of the glazed surface, the higher the permeability [6].

4.2. Characterization of the TiO_2 Coatings

The produced TiO_2 thin-films could be visually detected by the naked eye on the surface of the tile. They showed good adherence and were not detached to the touch nor by water immersion. The μ-Raman analysis confirmed the presence of the polymorphic anatase on all samples. This crystalline phase of TiO_2 is the most widely used for photocatalytic purposes [39,76]. Morphological and structural characterization of the coating showed good surface coverage and few surface flaws, like pores and large particles (Figure 3). The micro-fissures detected on the coating of some tile samples seemed to result from pre-existing fissures (Figure S1). The nanostructure of the TiO_2 film was similar to other sol-gel produced coatings, with cauliflower-shaped aggregates formed on the tiles' surface,

as previously described in the literature [77]. Similar morphological features were observed among all types of tiles studied in this work, indicating that sol-gel and spin-coating produced similar coatings on all tile samples.

4.3. Effect of TiO_2 Coatings on Tile Bioreceptivity

To test the efficacy of the deposited coatings, a tertiary bioreceptivity laboratory-based experiment was performed [30]. It was observed that the fungus *Cladosporium* sp. proliferated on all tile samples, both on the TiO_2-treated and non-treated ones. Nevertheless, fungal proliferation was lower on the TiO_2-coated samples, suggesting that the coating reduced tile bioreceptivity (Figures 5 and 6). The only exception was observed for the modern tile samples (4MW), where the fungal proliferation was higher on the treated samples (4MWT) than on the non-coated samples (4MW). In fact, these tiles depicted the highest surface colonization (Figure 6). After 40 days of incubation, a decrease in fungal growth could be percieved on all the samples (Figure 6), probably due to the consumption of the nutrients from the culture medium [8]. This decrease seemed more accentuated on the TiO_2-treated samples, which could be attributed to the photocatalytic effect of the TiO_2 nanoparticles. A previous study on mortars with TiO_2 additive showed good resistance against *Cladosporium* ssp. [78].

The results of previous studies showed that tile bioreceptivity to fungal colonization was in general reduced and seemed to indicate that fungal growth was strongly dependent on the presence of nutrients [79,80]. Thus, the use of a fast-growing fungus and higher nutrient concentration in the inoculum resulted in faster and more extensive growth than the results obtained on previous studies on glazed tiles [8]. A lower level of fungal proliferation occurred on samples with micro-fissures or cracks on the glaze. These results suggest that the amount of nutrients retained on samples without surface fissures was higher, promoting a higher level of fungal proliferation.

Further research should address the influence of the surface permeability, surface wettability and slope angle on the bioreceptivity of TiO_2-treated tiles. The slope angle may be a relevant factor when testing bioreceptivity and anti-biofouling properties, particularly on self-cleaning materials. In general, the deposited TiO_2 coatings slightly reduced tile bioreceptivity, but did not avoid the fungal proliferation on the surface of the tiles. In fact, other studies have also reported the inability of TiO_2 to prevent biological colonization [5]. However, nanoparticles are still a promising field for developing novel conservation materials [38]. Multiple solutions such as the combination of TiO_2 with other nanoparticles or the use of other particles, such as Cu, Ag, Zn might improve the efficacy of thin-coatings [38]. Yet, the impact of nanoparticles on the environment is still a major concern, particularly due to their effect on non-target organisms and their production processes [38]. Novel approaches are being tested for the reduction in the environmental impact of the production process. For instance, Estevez et al. [81] recently evaluated the use of biogenic Ag nanoparticles to eradicate biofilms, obtaining promising results. However, for the application of cultural heritage materials, the effect of the treatment on the substrate can be challenging.

4.4. Harmfulness Evaluation of TiO_2 Coatings on Historical Glazed Tiles

The TiO_2 coating induced aesthetic changes on all tile samples, which were evident by the iridescent colors on the tile surfaces (Figure 7a,b). Even though it is frequently claimed in the literature that the application of these coatings is not accompanied by visual alteration of the substrates [82,83]. However, Aversa et al. [31] reported similar aesthetic effects on semi-glazed historical tile coated with TiO_2. The depositions of the thin TiO_2 coating over the glazes resulted in iridescent surfaces and increased reflectivity due to optical interference (Figure 7). The reflection between parallel surfaces (in this case, TiO_2 coating and translucent glaze) generates optical interferences, like the ones described for self-cleaning glass [84]. These colored effects result in reflection amplitudes that depend on the light wavelength and film thickness, which in reflectance cause interference like iridescence and color. The increase in reflectivity observed on the coated samples has also been described on glass samples [84]. This increase may be related to the difference between the refraction index of TiO_2 and glass. For future

development of coatings to be applied on glazed tiles, the reflection index needs to be evaluated to reduce the optical interference-effect. Regardless of the aesthetical alterations on sample 1BW, staining and darkening were also observed. The TiO_2 coating and heat treatment probably induced chemical alteration of the substrate. Considering that dark stains were not detected on non-treated 1BW samples exposed to HNO_3 (Figure S2), lead corrosion products might have been reduced during thermal treatment into metallic lead. The blackening of lead glazes during the firing process can occur due to the reduction of lead oxide to its metallic form [85]. Further investigations need to be performed to understand the formation of these stains. To avoid chemical alterations, Bertoncello et al. [82] added small amounts of $Pb(NO_3)_2$ silica sol-gel coatings applied on lead glass. Regarding the effect of the coating application process (thermal treatment) on the ceramic body, XRD revealed no drastic changes on the mineral phase composition (Figure 9). However, small changes might not be detected. According to the thermal analysis of pottery, the main reactions that can be observed until 350 °C in calcareous ceramics are related to water loss by the dehydration and the beginning of de-hydroxylation of clay minerals [40]. In fact, the decarbonization reaction that could affect the high calcite content of samples 1BW and 2W only occurs at temperatures of around 750 °C [70]. However, further analysis should involve the characterization of the thermal expansibility to understand if the tensions created by the expansion and contraction of the glaze and ceramic body during thermal treatment can cause the decay of mechanical properties. The long-term performance, durability and reversibility of the studied treatment were not evaluated due to the aesthetical and chemical alterations observed during the experiment. Thus, future work should comprise the evaluation of the long-term performance of the coatings through accelerated aging or long-term on-site experiments. Since the lack of long-term evaluation of the behavior of these materials is still represents a barrier for their application [86]. For the in-situ application of the TiO_2 treatment on historical tiles, the need for thermal treatment of the sol-gel would represent a drawback. This could be overcome as the removal and remounting of tiles for the cleaning and renewal of aged mortars is a common procedure in historical tile conservation.

The application of glazed tiles in architecture is strongly related to an aesthetical intention [87]. Therefore, the alterations observed on the tile's surface after the application of TiO_2 coating suggest that the tested methodology is not suitable for glazed tiles from cultural heritage. The results also emphasize the importance of testing treatments for cultural heritage application in conditions as close as possible to real conditions regarding substrate characteristics and environmental conditions. However, the development of preventive coatings still represents a promising solution for protecting outdoor heritage against external threats.

5. Conclusions

Thin TiO_2 coating produced by the sol-gel method was tested on three historical glazed tiles and one modern tile to assess its anti-biofouling properties and to evaluate its suitability for cultural heritage application. The coating did not prevent fungal growth, although a slight reduction in the proliferation was observed for most of the samples. The bioreceptivity experiment also showed that the cracks on the glaze's surface influenced fungal growth, probably due to the different amounts of nutrients that remained on the surface.

The application of the TiO_2 thin-coating on the blue and white historical tile chemically affected the glaze and induced aesthetical alteration on all tested glazed tiles. Despite the promising features of the deposited TiO_2 coatings (good adherence, anatase crystalline structure and a small decrease in bioreceptivity), our results indicate that the tested TiO_2 coating is unsuitable for application on glazed tiles from cultural heritage due to chemical and aesthetical interferences with the substrate.

Still, our research proved to be valuable for understanding certain critical issues for the future development of protective coatings. Research must focus on coatings with a less aggressive pH, a lower thermal treatment and presenting better aesthetical properties. Future work also needs to address the reversibility and durability of the coatings. Many coatings currently under investigation, such as TiO_2 and SiO_2, are not reversible from glassy substrates. Therefore, novel reversible coating materials

may be a solution to overcome this limitation, as well as the development of coatings that can be applied in-situ.

Supplementary Materials: The following are available online at http://www.mdpi.com/2079-6412/10/12/1169/s1. Figure S1: Scanning electron microscopy images of the surface of the TiO_2-treated glazed tiles and Figure S2: Scanning electron microscopy images of the surface of glazed tile 1BW before and after 2 h exposure to HNO_3.

Author Contributions: Conceptualization, methodology, Investigation M.L.C., A.Z.M., J.P.V., and M.F.M.; writing—original draft preparation, M.L.C. and A.Z.M.; Manuscript review J.P.V. and M.F.M. All authors have read and agreed to the published version of the manuscript.

Funding: This research was funded by National Funds through FCT-Portuguese Foundation for Science and Technology (Fundação para a Ciência e Tecnologia) under the projects: UID/CTM/50025/2019 for I3N/FCT-UNL; UID/EAT/00729/2019 for VICARTE/FCT-UNL and UID/Multi/04449/2019 for HERCULES/UE, and Contracts CEECIND/00349/2017 to ML. Coutinho and CEECIND/01147/2017 to AZ. Miller.

Acknowledgments: The authors wish to acknowledge LAQV—REQUIMTE, Departamento de Química, Faculdade de Ciências e Tecnologia, Universidade Nova De Lisboa for supplying the materials and facilities for the experiment. Demolicões-Antunes, Lda. for the glazed tile samples. The authors would like to thank Isabel Nogueira from the MicroLab, Instituto Superior Técnico (University of Lisbon, Portugal) for the FESEM analysis.

Conflicts of Interest: The authors declare no conflict of interest.

References

1. De Carvalho, R.S. To be part of Architecture, decoration or iconography. Documenting azulejo as integrated heritage. *ISPRS Ann. Photogramm. Remote Sens. Spat. Inf. Sci.* **2019**, *4*, 39–46. [CrossRef]
2. Baricza, Á.; Bajnóczi, B.; Kovács, J.; May, Z.; Szabó, M.; Szabó, C.; Tóth, M. Chemical durability of lead-bearing glazes in sulphuric acid solutions—Laboratory experiments performed on Zsolnay architectural ceramics from Budapest (Hungary). *Int. J. Arch. Heritage* **2018**, *12*, 216–236. [CrossRef]
3. Baricza, Á.; Bajnóczi, B.; Szabó, M.; Tóth, M.; Bendo, Z.; Szabó, C. Deterioration of glazed architectural ceramics due to environmental factors: A comparative study of two buildings in Budapest. *Carpathian J. Earth Environ. Sci.* **2016**, *11*, 449–462.
4. Baricza, A.; Baknóczi, B.; Tóth, M.; Szabó, C. Deterioration of building ceramics by environmental factor–A case study on Zsolnay ceramics from the museum of applied arts (Budapest). In Proceedings of the Deterioration of Building Ceramics by Environmental Factors, Miskolc–Egyetemváros, Hungary, 27–29 September 2012.
5. Coutinho, M.L.; Miller, A.Z.; Martin-Sanchez, P.M.; Mirão, J.; Gomez-Bolea, A.; Machado-Moreira, B.; Cerqueira-Alves, L.; Jurado, V.; Saiz-Jimenez, C.; Lima, A.; et al. A multiproxy approach to evaluate biocidal treatments on biodeteriorated majolica glazed tiles. *Environ. Microbiol.* **2016**, *18*, 4794–4816. [CrossRef]
6. Coutinho, M.L.; Miller, A.Z.; Rogerio-Candelera, M.A.; Mirão, J.; Alves, L.C.; Veiga, J.P.; Águas, H.; Pereira, S.R.M.; Lyubchyk, A.; Macedo, M. An integrated approach for assessing the bioreceptivity of glazed tiles to phototrophic microorganisms. *Biofouling* **2016**, *32*, 243–259. [CrossRef]
7. Coutinho, M.; Miller, A.; Gutierrez-Patricio, S.; Hernández-Mariné, M.; Gomez-Bolea, A.; Rogerio-Candelera, M.; Philips, A.; Jurado, V.; Saiz-Jimenez, C.; Macedo, M. Microbial communities on deteriorated artistic tiles from Pena National Palace (Sintra, Portugal). *Int. Biodeterior. Biodegrad.* **2013**, *84*, 322–332. [CrossRef]
8. Coutinho, M.L.; Miller, A.; Phillip, A.; Mirão, J.; Dias, L.; Rogerio-Candelera, M.; Saiz-Jimenez, C.; Martin-Sanchez, P.; Cerqueira-Alves, L.; Macedo, M. Biodeterioration of majolica glazed tiles by the fungus Devriesia imbrexigena. *Constr. Build. Mater.* **2019**, *212*, 49–56. [CrossRef]
9. Oliveira, M.M.; Sanjad, T.B.C.; Bastos, C.J.P. Biological degradation of glazed ceramic tiles. In Proceedings of the Historical Constructions, Guimarães, Portugal, 7–9 November 2001; Lourenço, P.B., Roca, P., Eds.; pp. 337–342.
10. Giacomucci, L.; Bertoncello, R.; Salvadori, O.; Martini, I.; Favaro, M.; Villa, F.; Sorlini, C.; Cappitelli, F. Microbial Deterioration of Artistic Tiles from the Façade of the Grande Albergo Ausonia & Hungaria (Venice, Italy). *Microb. Ecol.* **2011**, *62*, 287–298. [CrossRef]

11. Verde, S.C.; Silva, T.; Corregidor, V.; Esteves, L.; Dias, M.; Souza-Egipsy, V.; Ascaso, C.; Wierzchos, J.; Santos, L.F.; Prudêncio, M.I. Microbiological and compositional features of green stains in the glaze of the Portuguese "Great View of Lisbon" tile panel. *J. Mater. Sci.* **2015**, *50*, 6656–6667. [CrossRef]
12. Coutinho, M.L.; Miller, A.Z.; Macedo, M.F. Biological colonization and biodeterioration of architectural ceramic materials: An overview. *J. Cult. Heritage* **2015**, *16*, 759–777. [CrossRef]
13. Caneva, G.; Nugari, M.P.; Salvadori, O. *Biology in the Conservation of Works of Art*; ICCROM: Rome, Italy, 1991; ISBN 9290771011.
14. Berti, S.; Pinzari, F.; Tiano, P. Control of biodeterioration and bioremediation techniques. Physical methods. In *Plant Biology for Cultural Heritage: Biodeterioration and Conservation*; Caneva, G., Nugari, M.P., Salvadori, O., Eds.; Getty Conservation Institute: Los Angeles, CA, USA, 2008; pp. 317–318.
15. Speranza, M.; Sanz, M.; Oujja, M.; Ríos, A.D.L.; Wierzchos, J.; Pérez-Ortega, S.; Castillejo, M.; Ascaso, C. Nd-YAG laser irradiation damages to Verrucaria nigrescens. *Int. Biodeterior. Biodegrad.* **2013**, *84*, 281–290. [CrossRef]
16. Tretiach, M.; Bertuzzi, S.; Carniel, F.C. Heat Shock Treatments: A New Safe Approach against Lichen Growth on Outdoor Stone Surfaces. *Environ. Sci. Technol.* **2012**, *46*, 6851–6859. [CrossRef]
17. Stupar, M.; Grbić, M.L.; Džamić, A.; Unković, N.; Ristić, M.; Jelikić, A.; Vukojević, J. Antifungal activity of selected essential oils and biocide benzalkonium chloride against the fungi isolated from cultural heritage objects. *S. Afr. J. Bot.* **2014**, *93*, 118–124. [CrossRef]
18. Mascalchi, M.; Osticioli, I.; Riminesi, C.; Cuzman, O.A.; Salvadori, B.; Siano, S. Preliminary investigation of combined laser and microwave treatment for stone biodeterioration. *Stud. Conserv.* **2015**, *60*, S19–S27. [CrossRef]
19. Caneva, G.; Nugari, M.P.; Salvadori, O. *Plant Biology for Cultural Heritage: Biodeterioration and Conservation*; Caneva, G., Nugari, M.P., Salvadori, O., Eds.; Getty Publ.: Los Angeles, CA, USA, 2008; ISBN 0892369396.
20. Silva, T.; Cabo Verde, S.; Burbidge, C.; Fernandes, A.; Botelho, M.; Dias, M.; Burbison, C.; Fernandes, A.; Botelho, M.; Dias, M. Perfis de contaminação e inactivação microbiana em azulejos. In Proceedings of the IX Congresso Ibérico de Arqueometria (CIA), Lisbon, Portugal, 26–28 October 2011; Fundação Caloust Gulbenkian: Lisbon, Portugal, 2011.
21. Russel, A.D.; Chopra, I. Understanding antibacterial action and resistance. *J. Med. Microbiol.* **1990**, *33*, 246. [CrossRef]
22. Pinna, D.; Galeotti, M.; Perito, B.; Daly, G.; Salvadori, B. In situ long-term monitoring of recolonization by fungi and lichens after innovative and traditional conservative treatments of archaeological stones in Fiesole (Italy). *Int. Biodeterior. Biodegrad.* **2018**, *132*, 49–58. [CrossRef]
23. Jurado, V.; Miller, A.; Cuezva, S.; Fernandez-Cortes, A.; Benavente, D.; Rogerio-Candelera, M.; Reyes, J.; Cañaveras, J.; Sanchez-Moral, S.; Saiz-Jimenez, C. Recolonization of mortars by endolithic organisms on the walls of San Roque church in Campeche (Mexico): A case of tertiary bioreceptivity. *Constr. Build. Mater.* **2014**, *53*, 348–359. [CrossRef]
24. Mendes, M.T.; Ferreira, T.A.; Candeias, A.; Rodrigues, J.D.; Mimoso, J.M.; Pereira, S.R.M. Volumetric and chromatic reintegration in conservation of in situ glazed tiles. In Proceedings of the Internantional Conferrence Glazed Ceramics in Architectural Heritage (GlazeArch2015), LNEC, Lisbon, Portugal, 2–3 July 2015; pp. 259–261, ISBN 978-972-49-2277-5.
25. Mendes, M.T.; Pereira, S.; Ferreira, T.; Mirão, J.; Candeias, A. In situ preservation and restoration of architectural tiles, materials and procedures: Results of an international survey. *Int. J. Conserv. Sci.* **2015**, *6*, 51–62.
26. Mendes, M.T.; Esteves, L.; Ferreira, T.; Candeias, A.; Tennent, N.H.; Rodrigues, J.D.; Pereira, S.R.M. Lacunae infills for in situ treatment of historic glazed tiles. *Appl. Phys. A* **2016**, *122*, 122. [CrossRef]
27. Pereira, S.R.M.; Musacchi, J.; Loureiro, J.; Cabral-fonseca, S.; Silva, H.; Rodrigues, M.P.M.C. Adhesives for Outdoor Architectural Historic Azulejo Conservation. In Proceedings of the Internantional Conferrence Glazed Ceramics in Architectural Heritage (GlazeArch2015), LNEC, Lisbon, Portugal, 2–3 July 2015; pp. 263–267, ISBN 978-972-49-2277-5.
28. Donà, V.; Cavallin, T.; Gambirasi, A.; Russo, U.; Nodari, L.; Bertoncello, R.; Favaro, M. A survey of polymeric treatments applied on the Liberty glazed tiles of the Hungaria façade. In Proceedings of the Hydrophobe VI: 6th International Conference on Water Repellent Treatments of Building Materials, Roma, Italy, 12–13 May 2011.
29. Pereira, S.R.M.; Esteves, L.; Rodrigues, J.; Mimoso, J.; Nacional, L.; Civil, D.E.; Esteves, L.; Nacional, M. Cerazul: Assessment and Development of Materials and Techniques for the Conservation of Historic Azulejos. In Proceedings of the Azulejar, Aveiro, Portugal, 10–12 October 2012; pp. 1–8, ISBN 978-989-98041-1-1.

30. Guillitte, O. Bioreceptivity: A new concept for building ecology studies. *Sci. Total Environ.* **1995**, *167*, 215–220. [CrossRef]
31. Aversa, R.; Perrotta, V.; Petrescu, R.V.; Carlo, M.; Petrescu, F.I.; Apicella, A. From Structural Colors to Super-Hydrophobicity and Achromatic Transparent Protective Coatings: Ion Plating Plasma Assisted TiO_2 and SiO_2 Nano-Film Deposition. *SSRN Electron. J.* **2017**. [CrossRef]
32. Mocioiu, O.C.; Mocioiu, A.-M.; Marin, A.; Zaharescu, M. Study of historical lead silicate glasses and their preservation by silica coating. *Ceram. Int.* **2017**, *43*, 77–83. [CrossRef]
33. Bianco, B.D.; Bertoncello, R. Sol–gel silica coatings for the protection of cultural heritage glass. *Nucl. Instrum. Methods Phys. Res. Sect. B Beam Interact. Mater. Atoms.* **2008**, *266*, 2358–2362. [CrossRef]
34. De Bardi, M.; Hutter, H.; Schreiner, P.M.; Bertoncello, R. Sol–gel silica coating for potash–lime–silica stained glass: Applicability and protective effect. *J. Non-Cryst. Solids* **2014**, *390*, 45–50. [CrossRef]
35. Kessler, V.G. *Handbook of Sol-Gel Science and Technology*; Springer: Berlin/Heidelberg, Germany, 2017; ISBN 9783319194547.
36. De Bardi, M.; Hutter, H.; Schreiner, P.M.; Bertoncello, R. Potash-lime-silica glass: Protection from weathering. *Heritage Sci.* **2015**, *3*, 101. [CrossRef]
37. Artesani, A.; Di Turo, F.; Zucchelli, M.; Traviglia, A. Recent Advances in Protective Coatings for Cultural Heritage–An Overview. *Coatings* **2020**, *10*, 217. [CrossRef]
38. Reyes-Estebanez, M.; Ortega-Morales, B.O.; Chan-Bacab, M.; Granados-Echegoyen, C.; Camacho-Chab, J.C.; Pereañez-Sacarias, J.E.; Gaylarde, C.C. Antimicrobial engineered nanoparticles in the built cultural heritage context and their ecotoxicological impact on animals and plants: A brief review. *Heritage Sci.* **2018**, *6*, 52. [CrossRef]
39. Kemmitt, T.; Al-Salim, N.; Waterland, M.; Kennedy, V.; Markwitz, A. Photocatalytic titania coatings. *Curr. Appl. Phys.* **2004**, *4*, 189–192. [CrossRef]
40. Markowska-Szczupak, A.; Ulfig, K.; Morawski, A. The application of titanium dioxide for deactivation of bioparticulates: An overview. *Catal. Today* **2011**, *169*, 249–257. [CrossRef]
41. Fujishima, A.; Zhang, X. Titanium dioxide photocatalysis: Present situation and future approaches. *Comptes Rendus Chim.* **2006**, *9*, 750–760. [CrossRef]
42. Goffredo, G.B.; Quagliarini, E.; Bondioli, F.; Munafo, P. TiO_2 nanocoatings for architectural heritage: Self-cleaning treatments on historical stone surfaces. *Proc. Inst. Mech. Eng. Part N J. Nanoeng Nanosyst.* **2013**, *228*, 2–10. [CrossRef]
43. Munafò, P.; Goffredo, G.B.; Quagliarini, E. TiO_2-based nanocoatings for preserving architectural stone surfaces: An overview. *Constr. Build. Mater.* **2015**, *84*, 201–218. [CrossRef]
44. Quagliarini, E.; Bondioli, F.; Goffredo, G.B.; Licciulli, A.; Munafò, P. Smart surfaces for architectural heritage: Preliminary results about the application of TiO2-based coatings on travertine. *J. Cult. Herit.* **2012**, *13*, 204–209. [CrossRef]
45. La Russa, M.F.; Ruffolo, S.A.; Rovella, N.; Belfiore, C.M.; Palermo, A.M.; Guzzi, M.T.; Crisci, G.M. Multifunctional TiO2 coatings for Cultural Heritage. *Prog. Org. Coat.* **2012**, *74*, 186–191. [CrossRef]
46. Fonseca, A.J.; Pina, F.; Macedo, M.; Leal, N.; Romanowska-Deskins, A.; Laiz, L.; Gómez-Bolea, A.; Saiz-Jimenez, C. Anatase as an alternative application for preventing biodeterioration of mortars: Evaluation and comparison with other biocides. *Int. Biodeterior. Biodegrad.* **2010**, *64*, 388–396. [CrossRef]
47. Bergamonti, L.; Predieri, G.; Paz, Y.; Fornasini, L.; Lottici, P.; Bondioli, F. Enhanced self-cleaning properties of N-doped TiO_2 coating for Cultural Heritage. *Microchem. J.* **2017**, *133*, 1–12. [CrossRef]
48. Franzoni, E.; Fregni, A.; Gabrielli, R.; Graziani, G.; Sassoni, E. Compatibility of photocatalytic TiO2-based finishing for renders in architectural restoration: A preliminary study. *Build. Environ.* **2014**, *80*, 125–135. [CrossRef]
49. Korkanç, M.; Savran, A. Impact of the surface roughness of stones used in historical buildings on biodeterioration. *Constr. Build. Mater.* **2015**, *80*, 279–294. [CrossRef]
50. Quagliarini, E.; Graziani, L.; Diso, D.; Licciulli, A.; D'Orazio, M. Is nano-TiO 2 alone an effective strategy for the maintenance of stones in Cultural Heritage? *J. Cult. Herit.* **2018**, *30*, 81–91. [CrossRef]
51. Graziani, L.; Quagliarini, E.; D'Orazio, M. TiO_2-treated different fired brick surfaces for biofouling prevention: Experimental and modelling results. *Ceram. Int.* **2016**, *42*, 4002–4010. [CrossRef]
52. García, L.Y.; Carrillo, M.F. El efecto migratorio en la asistencia escolar en Chile. *Estud. Pedagógicos (Valdivia)* **2019**, *45*, 47–59. [CrossRef]

53. Colangiuli, D.; Lettieri, M.; Masieri, M.; Calia, A. Field study in an urban environment of simultaneous self-cleaning and hydrophobic nanosized TiO_2-based coatings on stone for the protection of building surface. *Sci. Total Environ.* **2019**, *650*, 2919–2930. [CrossRef] [PubMed]
54. Mimoso, J.M. Cesare Brandi's Theory of Restoration of Azulejos. In Proceedings of the International Seminar on Conservation of Glazed Ceramic Tiles: Research and Practice, LNEC, Lisboa, Portugal, 15–16 April 2009; (CD-ROM). pp. 1–9.
55. Berto, A.M. Ceramic tiles: Above and beyond traditional applications. *J. Eur. Ceram. Soc.* **2007**, *27*, 1607–1613. [CrossRef]
56. Coentro, S.; Trindade, R.A.; Mirão, J.; Candeias, A.; Alves, L.C.; Silva, R.M.; Muralha, V.S. Hispano-Moresque ceramic tiles from the Monastery of Santa Clara-a-Velha (Coimbra, Portugal). *J. Archaeol. Sci.* **2014**, *41*, 21–28. [CrossRef]
57. Coentro, S.; Mimoso, J.M.; Lima, A.M.; Silva, A.S.; Pais, A.N.; Muralha, V.S. Multi-analytical identification of pigments and pigment mixtures used in 17th century Portuguese azulejos. *J. Eur. Ceram. Soc.* **2012**, *32*, 37–48. [CrossRef]
58. Van De Voorde, L.; Vandevijvere, M.; Vekemans, B.; Van Pevenage, J.; Caen, J.; Vandenabeele, P.; Van Espen, P.; Vincze, L. Study of a unique 16th century Antwerp majolica floor in the Rameyenhof castle's chapel by means of X-ray fluorescence and portable Raman analytical instrumentation. *Spectrochim. Acta Part B At. Spectrosc.* **2014**, *102*, 28–35. [CrossRef]
59. Eppler, R. Corrosion of Glazes and Enamels. In *Corrosion of Glass, Ceramics and Ceramic Superconductors*; Clark, D., Zoitos, B., Eds.; Noyes Publications: Park Ridge, IL, USA, 1992.
60. Maver, K.; Štangar, U.L.; Cernigoj, U.; Gross, S.; Korošec, R.C. Low-temperature synthesis and characterization of TiO_2 and TiO_2–ZrO_2 photocatalytically active thin films. *Photochem. Photobiol. Sci.* **2009**, *8*, 657–662. [CrossRef]
61. Coutinho, M.L.; Pinheiro, C.; Phillips, A.; Macedo, M. Biodeterioration of tiles from Pena National Palace (Portugal). First step: Identification of fungal community. In Proceedings of the 16th Triennial Meeting on ICOM-CC, Lisbon, Portugal, 19–23 September 2011; p. 82.
62. Sekiya, T.; Ohta, S.; Kamei, S.; Hanakawa, M.; Kurita, S. Raman spectroscopy and phase transition of anatase TiO_2 under high pressure. *J. Phys. Chem. Solids* **2001**, *62*, 717–721. [CrossRef]
63. Vaz, M.; Fernandes, A.C.; Carvalho, A. Effect of the impregnation treatment with Paraloid B-72 on the properties of old Portuguese ceramic tiles. *J. Cult. Herit.* **2008**, *9*, 269–276. [CrossRef]
64. Pereira, S.R.M.; Esteves, L.; Mendes, M.T.; Musacchi, J.; Rodrigues, J.D.; Mimoso, J.M.; Esteves, L.; Mendes, M.T.; Musacchi, J.; Rodrigues, J.D.; et al. Degradation forms of historical Portuguese tiles under accelerated salt ageing. In Proceedings of the Azulejar, Aveiro, Portugal, 10–12 October 2012; pp. 1–10, ISBN 978-989-98041-1-1.
65. Prudêncio, M.I.; Pereira, M.A.S.; Marques, J.; Dias, M.; Esteves, L.; Burbidge, C.; Trindade, M.J.; Albuquerque, M. Neutron tomography for the assessment of consolidant impregnation efficiency in Portuguese glazed tiles (16th and 18th centuries). *J. Archaeol. Sci.* **2012**, *39*, 964–969. [CrossRef]
66. Ottosen, L.M.; Dias-Ferreira, C.; Ribeiro, A. Electrochemical desalination of historic Portuguese tiles – Removal of chlorides, nitrates and sulfates. *J. Cult. Herit.* **2015**, *16*, 712–718. [CrossRef]
67. Pereira, S.; Mimoso, J.M.; Santos Silva, A. *RELATÓRIO 23/2011 Physical-Chemical Characterization of Historic Portuguese Tiles*; Laboratório Nacional de Engenharia Civil: Lisbon, Portugal, 2011.
68. Rede de Investigação em Azulejo Az Infinitum—Sistema de Referência e Indexação de Azulejo. Available online: http://redeazulejo.letras.ulisboa.pt/pesquisa-az/integrado.aspx?id=3680 (accessed on 9 June 2020).
69. Jordán, M.M.; Montero, M.; Meseguer, S.; Sanfeliu, T. Influence of firing temperature and mineralogical composition on bending strength and porosity of ceramic tile bodies. *Appl. Clay Sci.* **2008**, *42*, 266–271. [CrossRef]
70. Fabbri, B.; Gualtieri, S.; Shoval, S. The presence of calcite in archeological ceramics. *J. Eur. Ceram. Soc.* **2014**, *34*, 1899–1911. [CrossRef]
71. Eggert, G. To whom cracks tell: A closer look at craquelure in glass and glaze. *Stud. Conserv.* **2006**, *51*, 69–75. [CrossRef]
72. González-García, F.; Romero-Acosta, V.; García-Ramos, G.; González-Rodríguez, M. Firing transformations of mixtures of clays containing illite, kaolinite and calcium carbonate used by ornamental tile industries. *Appl. Clay Sci.* **1990**, *5*, 361–375. [CrossRef]

73. Assunção, A.P.; Pereira, C.; Correia, E. *Primeiras Peças da Produção da Fábrica de Loiça de Sacavém—O Papel do Coleccionador*; Sacavém, M., Ed.; Camara Mun.: Loures, Portugal, 2003.
74. Raimondo, M.; Dondi, M.; Mazzanti, F.; Stefanizzi, P.; Bondi, P. Equilibrium moisture content of clay bricks: The influence of the porous structure. *Build. Environ.* **2007**, *42*, 926–932. [CrossRef]
75. Belgaied, J.-E. Release of heavy metals from Tunisian traditional earthenware. *Food Chem. Toxicol.* **2003**, *41*, 95–98. [CrossRef]
76. Awitor, K.; Rivaton, A.; Gardette, J.-L.; Down, A.; Johnson, M. Photo-protection and photocatalytic activity of crystalline anatase titanium dioxide sputter-coated on polymer films. *Thin Solid Films* **2008**, *516*, 2286–2291. [CrossRef]
77. Alzamani, M.; Shokuhfar, A.; Eghdam, E.; Mastali, S. Influence of catalyst on structural and morphological properties of TiO_2 nanostructured films prepared by sol–gel on glass. *Prog. Nat. Sci.* **2013**, *23*, 77–84. [CrossRef]
78. Jerónimo, A.; Camões, A.; Barroso-Aguiar, J.L.; Lima, N. Hydraulic lime mortars with antifungal properties. *Appl. Surf. Sci.* **2019**, *483*, 1192–1198. [CrossRef]
79. Gadd, G.M.; Ramsay, L.; Crawford, J.W.; Ritz, K. Nutritional influence on fungal colony growth and biomass distribution in response to toxic metals. *FEMS Microbiol. Lett.* **2001**, *204*, 311–316. [CrossRef] [PubMed]
80. Giannantonio, D.J.; Kurth, J.C.; Kurtis, K.E.; Sobecky, P.A. Effects of concrete properties and nutrients on fungal colonization and fouling. *Int. Biodeterior. Biodegrad.* **2009**, *63*, 252–259. [CrossRef]
81. Estevez, M.B.; Raffaelli, S.; Mitchell, S.G.; Faccio, R.; Albores, S. Biofilm Eradication Using Biogenic Silver Nanoparticles. *Molecules* **2020**, *25*, 2023. [CrossRef] [PubMed]
82. Bertoncello, R.; Milanese, L.; Dran, J.C.; Bouquillon, A.; Sada, C. Sol–gel deposition of silica films on silicate glasses: Influence of the presence of lead in the glass or in precursor solutions. *J. Non-Cryst. Solids* **2006**, *352*, 315–321. [CrossRef]
83. Murugan, K.; Subasri, R.; Rao, T.; Gandhi, A.S.; Murty, B.S. Synthesis, characterization and demonstration of self-cleaning TiO_2 coatings on glass and glazed ceramic tiles. *Prog. Org. Coat.* **2013**, *76*, 1756–1760. [CrossRef]
84. Tilley, R.J.D. *Colour and The Optical Properties of Materials*; John Wiley & Sons: Hoboken, NJ, USA, 2010; ISBN 978-0-470-74696-7.
85. Tite, M.S.; Freestone, I.; Mason, R.; Molera, J.; Vendrell-Saz, M.; Wood, N. Lead glazes in antiquity? Methods of production and reasons for use. *Archaeometry* **1998**, *40*, 241–260. [CrossRef]
86. Ruffolo, S.A.; La Russa, M.F. Nanostructured Coatings for Stone Protection: An Overview. *Front. Mater.* **2019**, *6*, 6. [CrossRef]
87. Lobo, C.; Pernão, J. Glazed tiles as an improving element for environmental quality in Urban Landscape. *J. Int. Colour Assoc.* **2010**, *9*, 1–12.